ChemComm

COMMUNICATION

View Article Online
View Journal | View Issue

Cite this: *Chem. Commun.*, 2026, **62**, 5068

Received 13th January 2026,
Accepted 9th February 2026

DOI: 10.1039/d6cc00180g

rsc.li/chemcomm

A new strain-crystallizable rubber *via* neodymocene-catalyzed regio-, stereo-, and sequence-selective copolymerization of isoprene and ethylene

Jingqing Lyu, [a] Zhenxing Chen, [b] Lei Zhu *[b] and Li Jia *[a]

An ansa-neodymocene catalyst previously reported in the literature has been identified to catalyze the title copolymerization to afford poly(1,4-*trans*-isoprene–ethylene) with 95% selectivity for the major microstructure. Such structural regularity is minimally required for the rubbery product, dubbed isoprene–ethylene rubber (IER), to exhibit prominent strain-induced crystallization (SIC) at 0 °C. The mechanical properties of IER rival those of natural rubber when SIC occurs. The unit cell of the strain-induced crystals is monoclinic with *a* = 2.21 nm, *b* = 0.72 nm, *c* = 1.30 nm, and *β* = 110.8°. Each unit cell is estimated to contain 12 chains in the *ac* plane and one repeat unit along the *b* axis.

Strain-induced crystallization (SIC) is a fascinating phenomenon of enormous practical importance for elastomers. For traditional applications based on mechanical and dynamic mechanical properties, the crystals that form when the elastomer is under a mechanical strain reinforce the elastic network by slowing crack growth and deflecting catastrophic crack propagation without causing viscous dissipation.[1] This makes natural rubber (NR), which undergoes rapid SIC to an unmatched degree, irreplaceable for applications that require high tear resistance. Contemporary novel applications such as elastocaloric cooling[2] and strain-programmable actuation[3] exploit other physical consequences that the SIC phenomenon brings. For applications that require elastic recovery (*e.g.*, elastocaloric cooling), NR remains the gold standard.[4]

Strong incentives exist to discover new elastomers that undergo SIC similar to or even better than NR but have structures different from NR and more broadly not in the poly(1,4-diene) family. From the viewpoint of traditional applications, NR and its synthetic counterpart known as isoprene rubber (IR) are prone to oxidative,[5] mechanical,[6] and mechano-oxidative chain scissions,[7] due to their high degree of unsaturation and the particular placement of the tertiary carbons in two consecutive 1,4-isoprene repeat units,[7] resulting in processing restrictions, mediocre abrasion resistance, and poor ageing in air. The new applications pose new challenges for elastic SIC materials. In particular, a high melt enthalpy is advantageous for elastocaloric cooling, but NR has an unusually low specific melt enthalpy.[8]

The literature on SIC is voluminous. Much of the focus has been placed on the effect of network structure on SIC[9] with the experimental works often using NR and IR as examples.[10–12] Very few touched upon the fundamental question of "What chemical structure gives rise to strong SIC for rubbers? "[8,9] For the present exercise of developing new SIC rubbers that are not in the poly(1,4-diene) family,[13–15] we found poly(1,4-*trans*-butadiene-*alt*-iso-propylene) an intriguing lead. The elastomer, named propylene–butadiene rubber (PBR) by Furukawa, who discovered it in 1969[16] using a vanadium-based Ziegler–Natta catalyst (eqn (1)), showed better strength than NR at 0 °C. It drew considerable interest from both industry and academics in the ensuing ten years.[17–20] Although the polymerization was carried out at −45 °C and the stereoregularity of the product was likely far from being perfect, attempts to improve the copolymerization involving a 4-fold selectivity based on Ziegler–Natta catalysts proved futile. It appears reasonable to postulate that the isomers of PBR, poly(1,4-*trans*-isoprene-*alt*-ethylene) (eqn (2)) or its *cis*-counterpart, are also likely candidates for SIC. Without the tacticity issue, the synthetic task is less formidable. We thus became interested in realizing the copolymerization using "single-site" catalysts,[21] which permit rational improvement once the initial discovery is made.

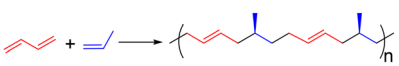
(1)

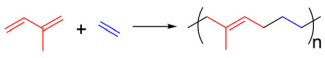
(2)

Several reports on the copolymerization of isoprene and ethylene exist in the literature,[22–29] but none came close to the selectivity for the product depicted by eqn (2) or its *cis*

[a] *School of Polymer Science and Polymer Engineering, The University of Akron, Akron, Ohio 44325-3909, USA. E-mail: ljia@uakron.edu*
[b] *Department of Macromolecular Science and Engineering, Case Western Reserve University, Cleveland, Ohio 44106-7202, USA. E-mail: lxz121@case.edu*

counterpart. This is in contrast to analogous alternating 1,3-butadiene–ethylene copolymerization, which has been known since the early days of Ziegler–Natta catalysis to produce the semicrystalline poly(1,4-*trans*-butadiene–ethylene).[30] The clearest lead to a catalyst for the target copolymerization came from the study of Carpentier and his coworkers on isoprene–ethylene–styrene terpolymerization.[31] An experiment of copolymerization catalyzed by **1** in neat isoprene and under 4 bars of ethylene without styrene was reported to give a copolymer without repetitive ethylene units. This suggests that the reactivity ratio of ethylene against isoprene is very small and that it may be possible to realize alternating copolymerization by adjusting the comonomer concentrations. Related to this, Boisson and coworkers reported that **2** activated by dialkylmagnesium produced poly(1,4-*trans*-butadiene-*alt*-ethylene) with high selectivity.[32]

In this communication, we report the successful achievement of the regio-, stereo-, and sequence-selective copolymerization of isoprene and ethylene taking advantage of the aforementioned existing single-site neodymocene catalysts. Initial investigations on SIC of the products, which we will refer to as isoprene–ethylene rubber (IER), show that prominent SIC occurs only when the selectivity for the 1,4-*trans*-isoprene–ethylene repeat unit reaches 95 mol%. The unit cell of strain-crystallized IER has been preliminarily identified. The remarkable effect of SIC on the mechanical properties of IER will be reported.

Catalysts **1–3** are explored with the aim of obtaining an alternating copolymer with optimal regio- and stereoregularity as well as a high molecular weight sufficient for forming a highly extensible elastic network upon crosslinking. The results are summarized in Table 1. The structures of the products were characterized by ^{1}H and ^{13}C NMR spectroscopies (Fig. 1 and Fig. S1). The abundances of the microstructures are determined by quantitative $^{13}C\{^{1}H\}$ NMR using the inverse-gated ^{1}H-decoupling technique (see the SI for details). The major repeat unit is 1,4-*trans*-isoprene–ethylene, and the second most abundant is 3,4-isoprene–ethylene in all cases. The molecular weights and polydispersity are determined by GPC relative to monodisperse polystyrene standards.

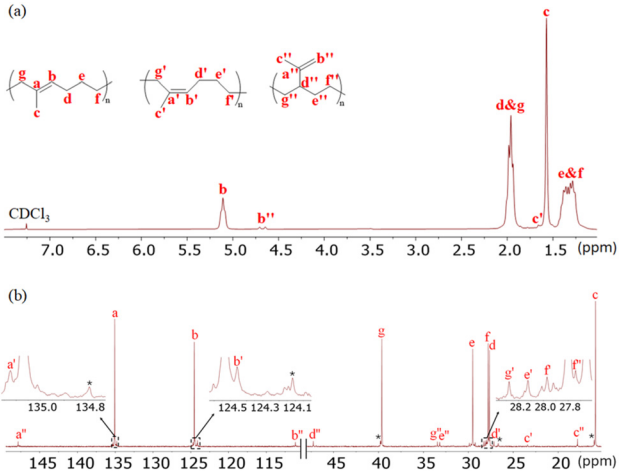

Fig. 1 ^{1}H and $^{13}C\{^{1}H\}$ NMR spectra of the products from entry 6 (IER-95) in Table 1 in $CDCl_3$ at room temperature. The ^{13}C peaks are assigned according to the literature.[25] The peaks labeled with an asterisk belong to repetitive isoprene units.

Under 550 psi of ethylene in neat isoprene (entry 1, Table 1), **1** produces a copolymer with >98% alternating sequence, but only ~82% of the repeat units are 1,4-*trans*-isoprene–ethylene. Attempts to improve the selectivity by lowering the polymerization temperature from 85 °C to 20 °C resulted in a decrease in the regioregularity (entry 2, Table 1). Catalyst **2** is initially activated by 5 eq. of Bu_2Mg as reported by Boisson. The selectivity of **2**/Bu_2Mg (5 eq.) is much better at 20 °C (entry 3) than at 80 °C (entry 4) for the desired microstructure. Only 100 psi of ethylene pressure is necessary for **2**/Bu_2Mg to produce a copolymer with >98% alternating selectivity at 20 °C (entry 3). Reducing Bu_2Mg from 5 eq. to 1 eq. results in a significant increase in molecular weight and slight improvements of selectivity and yield (entries 3 *vs.* 5). Further reducing Bu_2Mg to 0.5 eq. harms the selectivity and activity (entries 5 *vs.* 6). The analogous **3**/Bu_2Mg affords an alternating copolymer under 400 psi of ethylene (entry 7), but its selectivity is inferior to **2**/Bu_2Mg (entries 5 *vs.* 7).

Table 1 Summary of copolymerization of isoprene and ethylene[a]

Entry	Cat.	Bu_2Mg (eq)	Time (h)	Temp. (°C)	P_E (psi)	Yield (g)	*alt*-*trans*/*cis*/3,4[b] (mol%)	Repetitive isoprene[b] (mol%)	M_n[c] (kg mol^{-1})	$Đ$[c]
1	**1**	—	1	85	550	8.1	82.3/4.6/11.7	1.4	138	2.8
2	**1**	—	16	20	550	4.4	70.6/4.6/23.3	1.5	110	2.7
3	**2**	5.00	72	20	100	8.8	94.2/1.8/2.4	1.6	25	1.2
4	**2**	5.00	1	80	100	2.5	69.0/2.0/8.3	20.7	13	1.4
5	**2**	1.05	72	20	100	9.0	95.0/1.1/2.4	1.5	105	1.7
6	**2**	0.5	72	20	100	3.0	91.1/1.7/5.9	1.3	78	1.5
7	**3**	1.05	48	20	400	4.8	89.3/2.3/7.4	1.0	131	2.1

[a] Condition: **1** (~0.2 mmol), **2** (~0.07 mmol), or **3** (~0.07 mmol) in neat isoprene (6.8 g for **1** and **2**; 3.4 g for **3**). [b] Determined by quantitative $^{13}C\{^{1}H\}$ NMR. [c] Determined by GPC in THF *vs.* polystyrene standards.

In the subsequent discussion of physical and mechanical properties, we will focus on the product with the highest structural regularity from entry 5 (IER-95) and use the one from entry 7 (IER-89) for comparison. Both are amorphous at room temperature with the glass transition temperature (T_g) at −69.8 °C for IER-89 and −74.5 °C for IER-95 (Fig. S2). IER-95 shows two endothermal peaks at −23.5 and −3.8 °C after being held isothermally at −40 °C for 4 h (Fig. S3), but such features were absent in continuous DSC scans. The endotherms are attributable to melting of crystal lamellas of different thicknesses or unit cells, or even mesoscopic structures lacking long-range order. No crystallization was observed under any conditions for IER-89 apparently due to its insufficient stereoregularity.

For the initial exploration of possible SIC of IER, we adopted Gent's method of monitoring stress relaxation for its simplicity.[33,34] The validity of the method was established by the agreement between the experimentally observed proportionality of the degree of crystallization and the amount of relaxed stress with that derived from the theory of Flory.[33] Peroxide-cured IER-95 with a density of elastically effective strands (ν = 53.3 mol m^{-3}) that matches those of NR and IR (ν = 56.4 and 57.9 mol m^{-3}, respectively) studied by Gent[34] was used. The IER-95 sample begins to display pronounced SIC at 600% strain and 0 °C (Fig. 2a). The half-life of SIC ($\tau_{1/2}$), which is estimated as the time for stress to decrease by 50%, is 5.6 h at 0 °C under 600% strain. The melting temperature (T_m), which is taken as the temperature for the stress to reach a plateau upon warming the strain-crystallized sample (Fig. 2b), is ∼35 °C under 600% strain. No SIC was detected for IER-95 at room temperature or under strains < 600% at 0 °C. At −25 °C, $\tau_{1/2}$ of IER-95 is 2.1 h under 200% strain and 0.1 h under 600% strain, and the corresponding T_m is ∼6 °C and ∼16 °C under the respective strains. The observed changes in $\tau_{1/2}$ and T_m with changes in the crystallization temperature and strain level are characteristic of SIC. A comparison of IER-95 with IR and NR[34] for their SIC at −25 °C under 200% strain proves interesting. Although the T_m of IER-95 is markedly lower than that of IR (6 *vs.* 25 °C), IER-95 undergoes SIC faster than IR ($\tau_{1/2}$ = 2.1 *vs.* 3.3 h). A high SIC rate is known to be desirable for preventing mechanical failure as our study confirms (*vide infra*). Compared to NR ($\tau_{1/2}$ = 0.8 h and T_m = 30 °C), IER-95 is inferior in both aspects. No SIC is detectable for IER-89 with a similar density of elastically effective strands (ν = 57.7 mol m^{-3}) under such conditions, underlining the necessity of structural regularity for IER to undergo SIC.

Wide-angle X-ray diffraction (WAXD) studies were carried out on thermally crystallized and strain-crystallized IER-95. The unstretched sample was kept at −40 °C for 4 h before the X-ray data were collected at the same temperature. Although melt-like transitions are observable by DSC after isothermal annealing under the same conditions (*vide supra*), diffractions are very weak amidst the amorphous halo and are only discernible in the 1-dimensional intensity plot at 2θ = 9.02°, 24.89°, and 27.40° (Fig. S4). The weakness of these signals suggests a lack of long-range order. In contrast, diffraction arcs are clearly observed from IER-95 stretched to various strains at −25 °C (Fig. 3a and Fig. S5). The 2θ values of the diffractions (see Table S2) are the same for samples at different strains but are different from those of the three vague diffraction rings of the unstretched sample. The 2-dimensional WAXD pattern of the sample stretched to 800% strain after Fraser correction was satisfactorily fitted with a monoclinic unit cell with a = 2.21 nm, b = 0.72 nm, c = 1.30 nm, and β = 110.8°. The reflections are indexed as shown in Fig. 3b (see Table S2 for the observed and calculated d-spacings). The b-axis is aligned in the uniaxial stretching direction and has a dimension corresponding to the estimated length of one repeat unit of IER with all single bonds adopting the anti conformation and the double bond in the *trans* configuration. If we assume a mass density of 1.0 g cm^{-3} for the crystal, the unit cell is estimated to contain 12 chains in the *ac* plane.

Tensile properties of IER-95 were studied at room temperature and 0 °C and compared with those of NR, IR, and IER-89 crosslinked to a similar degree (ν = 53–58 mol m^{-3}). At room temperature, IER-95 does not exhibit strain-hardening caused by SIC as NR and IR do (Fig. 4a), but the stress–strain curve of IER-95 transforms dramatically at 0 °C to include a prominent strain-hardening process (Fig. 4b). The strength and extensibility of IER-95 both substantially rise above those of IR (Table S3). Compared to NR at 0 °C, IER-95 remains weaker but is substantially more extensible, and the overall toughness (*i.e.*, the area under the stress–strain curve) of IER-95 is slightly better as a result (56.6 ± 2.6 *vs.* 49.3 ± 3.2 MJ m^{-3}). The

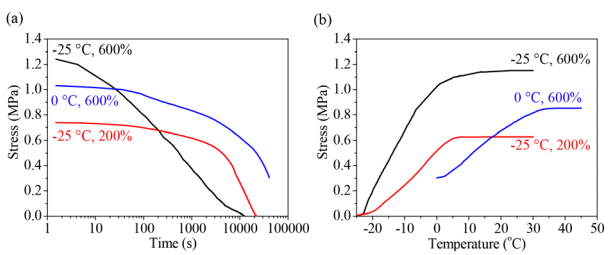

Fig. 2 (a) Stress relaxation of IER-95 at 0 and −25 °C. (b) Stress recovery with temperature increases at 200% strain and 600% strain after crystallization of 0 and −25 °C. The temperature ramp was 1 °C min^{-1}.

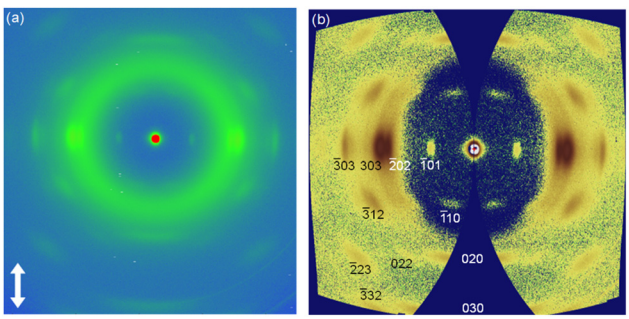

Fig. 3 X-ray study of IER-95 at 800% strain and −25 °C. (a) 2-Dimensional pattern without correction. The arrow indicates the stretching direction. (b) 2-Dimensional pattern with Fraser correction after subtraction of the amorphous background obtained with an unstretched sample.

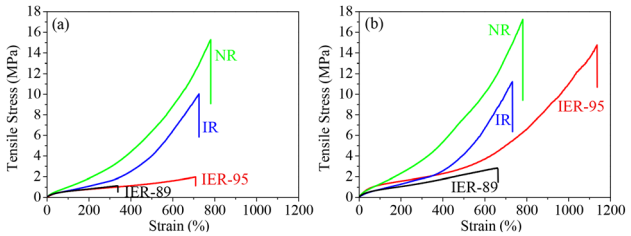

Fig. 4 Stress–strain curves of IER-89, IER-95, NR, and IR at room temperature (a) and 0 °C (b). The strain rate was 20% min^{-1}.

observed dramatic differences of IER-95 between room temperature and 0 °C are consistent with the SIC study, *i.e.*, SIC is not detectable at room temperature for IER-95 but becomes prominent at 0 °C under 600% strain. The stress–strain curves of IER-89 at room temperature and 0 °C show the typical temperature dependence of the mechanical properties of amorphous rubbers. The improvement of the mechanical properties of IER-95 is therefore mainly attributable to SIC.

In summary, we have successfully realized regio-, stereo-, and sequence-selective isoprene–ethylene co-polymerization. Achieving 95% selectivity for the major microstructure proves crucial for demonstrating that IER indeed undergoes SIC. The currently achieved molecular weight is also likely the minimum for demonstrating SIC of the new elastomer. SIC of IER-95 brings about mechanical properties superior to those of IR and rivalling those of NR at 0 °C. Further improvement of the structural regularity is necessary to raise the onset temperature of SIC for IER to become practically important. Development of new catalysts is ongoing in our laboratory. The 1,4-*trans*-isoprene–ethylene structure of IER suggests that it should have a smaller molecular weight between entanglements, a greater Kuhn length, and a greater degree of conformational freedom than NR and IR as well as a different melt enthalpy. These characteristics of IER may prove advantageous for SIC and afford an opportunity to answer the question "What chemical structure gives a supreme strain-crystallizable rubber?"

Conflicts of interest

The authors declare no conflicts of interest.

Data availability

Experimental procedures and additional characterization data are available in the supplementary information (SI) and upon request. Please send the request to the corresponding author. Supplementary information is available. See DOI: https://doi.org/10.1039/d6cc00180g.

Acknowledgements

We thank ACS PRF (66194-ND7) and NSF (DMR-2500507) for supporting the research.

References

1 A. Gent, *Science and technology of rubber*, Elsevier, 2005, pp. 455–495.
2 F. Greibich, *et al.*, Elastocaloric heat pump with specific cooling power of 20.9 W g^{-1} exploiting snap-through instability and strain-induced crystallization, *Nat. Energy*, 2021, **6**, 260–267.
3 C. Lang, *et al.*, Nanostructured block copolymer muscles, *Nat. Nanotechnol.*, 2022, **17**, 752–758.
4 C. M. Hartquist, *et al.*, An elastomer with ultrahigh strain-induced crystallization, *Sci. Adv.*, 2023, **9**, eadj0411.
5 J. R. Shelton, Review of basic oxidation processes in elastomers, *Rubber Chem. Technol.*, 1972, **45**, 359–380.
6 W. Watson, Cold mastication of rubber, *Rubber Chem. Technol.*, 1953, **26**, 377–385.
7 A. Casale, R. S. Porter and J. F. Johnson, The mechanochemistry of high polymers, *Rubber Chem. Technol.*, 1971, **44**, 534–577.
8 A. Gent, *Advances in elastomers and rubber elasticity*, Springer, 1986, pp. 253–267.
9 P. J. Flory, Thermodynamics of crystallization in high polymers. I. Crystallization induced by stretching, *J. Chem. Phys.*, 1947, **15**, 397–408.
10 S. Toki, *et al.*, Entanglements and networks to strain-induced crystallization and stress–strain relations in natural rubber and synthetic polyisoprene at various temperatures, *Macromolecules*, 2013, **46**, 5238–5248.
11 J.-M. Chenal, L. Chazeau, L. Guy, Y. Bomal and C. Gauthier, Molecular weight between physical entanglements in natural rubber: A critical parameter during strain-induced crystallization, *Polymer*, 2007, **48**, 1042–1046.
12 S. Trabelsi, P.-A. Albouy and J. Rault, Crystallization and melting processes in vulcanized stretched natural rubber, *Macromolecules*, 2003, **36**, 7624–7639.
13 C. R. López-Barrón, B. Rohde, A. V. Zabula, J. J. Schaefer and J. A. Throckmorton, Molecular orientation and strain-induced crystallization in *trans*-polypentenamer, *Macromolecules*, 2020, **53**, 1356–1367.
14 P. Xu and J. Mark, Strain-induced crystallization in elongated polyisobutylene elastomers, *Polym. Gels Networks*, 1995, **3**, 255–266.
15 X. Zhang, *et al.*, Comparative study on the molecular chain orientation and strain-induced crystallization behaviors of HNBR with different acrylonitrile content under uniaxial stretching, *Polymer*, 2021, **219**, 123520.
16 J. Furukawa, R. Hirai and M. Nakaniwa, An alternating copolymer of butadiene and propylene, *J. Polym. Sci., Part B: Polym. Lett.*, 1969, **7**, 671–678.
17 J. Furukawa, Stereoregular and sequence-regular polymerization of butadiene, *Acc. Chem. Res.*, 1980, **13**, 1–6.
18 C. J. Carman, The Determination of an Alternating Monomer Sequence Distribution in Propylene-Butadiene Copolymers Using Carbon-13 Nuclear Magnetic Resonance, *Macromolecules*, 1974, **7**, 789–793.
19 W. Wieder, H. Kroemer and J. Witte, Alternating copolymers of butadiene and propylene: Properties and characterization, *J. Appl. Polym. Sci.*, 1982, **27**, 3639–3649.
20 W. Wieder and J. Witte, Improved coordination catalyst for the alternating copolymerization of butadiene and propylene, *J. Appl. Polym. Sci.*, 1981, **26**, 2503–2508.
21 J. A. Gladysz, Thematic Issue: Frontier in metal-catalyzed polymerization, *Chem. Rev.*, 2000, **100**, 1167–1682.
22 L. Myagkova, Y. N. Kropacheva and A. Khachaturov, The synthesis and structure of alternating copolymers of isoprene with ethylene, *Polym. Sci. USSR*, 1984, **26**, 1063–1072.
23 T. Nishiyama and A. Ogawa, *US Pat.*, 6288191, 2001.
24 X. Li, M. Nishiura, L. Hu, K. Mori and Z. Hou, Alternating and random copolymerization of isoprene and ethylene catalyzed by cationic half-sandwich scandium alkyls, *J. Am. Chem. Soc.*, 2009, **131**, 13870–13882.
25 C. Capacchione, D. Saviello, A. Avagliano and A. Proto, Copolymerization of ethylene with isoprene promoted by titanium complexes containing a tetradentate [OSSO]-type bis (phenolato) ligand, *J. Polym. Sci., Part A: Polym. Chem.*, 2010, **48**, 4200–4206.
26 T. Chenal and M. Visseaux, Combining polyethylene CCG and stereoregular isoprene polymerization: first synthesis of Poly (ethylene)-*b*-(*trans*-isoprene) by neodymium catalyzed sequenced copolymerization, *Macromolecules*, 2012, **45**, 5718–5727.

27 S. Song, *et al.*, Trans-1, 4-stereospecific copolymerization of ethylene and isoprene catalyzed by MgCl2-supported Ziegler–Natta catalyst, *J. Polym. Sci., Part A: Polym. Chem.*, 2018, **56**, 2715–2722.
28 L. Guo, *et al.*, Synthesis of ethylene/isoprene copolymers containing cyclopentane/cyclohexane units as unique elastomers by half-titanocene catalysts, *Macromolecules*, 2023, **56**, 899–914.
29 A. Ali, *et al.*, Copolymerization of ethylene and isoprene via silicon bridge metallocene [rac-Me2Si (2-Me-4-Ph-Ind)2ZrCl2] catalyst: A new way to control the composition and microstructure of copolymers, *Chemosphere*, 2024, **347**, 140700.
30 G. Natta, A. Zambelli, I. Pasquon and F. Ciampelli, Crystalline alternating ethylene-butadiene copolymers, *Makromol. Chem.*, 1964, **79**, 161–169.
31 A.-S. Rodrigues, E. Kirillov, B. Vuillemin, A. Razavi and J.-F. Carpentier, Stereocontrolled styrene–isoprene copolymerization and styrene–ethylene–isoprene terpolymerization with a single-component allyl ansa-neodymocene catalyst, *Polymer*, 2008, **49**, 2039–2045.
32 J. Thuilliez, V. Monteil, R. Spitz and C. Boisson, Alternating copolymerization of ethylene and butadiene with a neodymocene catalyst, *Angew. Chem.*, 2005, **117**, 2649–2652.
33 A. Gent, Crystallization and the relaxation of stress in stretched natural rubber vulcanizates, *Trans. Faraday Soc.*, 1954, **50**, 521–533.
34 A. Gent, S. Kawahara and J. Zhao, Crystallization and strength of natural rubber and synthetic *cis*-1, 4-polyisoprene, *Rubber Chem. Technol.*, 1998, **71**, 668–678.

